Journal of Catalysis 261 (2009) 137–149

Contents lists available at ScienceDirect

Journal of Catalysis

www.elsevier.com/locate/jcat

CO oxidation catalyzed by gold supported on MgO: Spectroscopic identification of carbonate-like species bonded to gold during catalyst deactivation

Y. Hao [a], M. Mihaylov [b,c], E. Ivanova [c], K. Hadjiivanov [c], H. Knözinger [b], B.C. Gates [a,*]

[a] Department of Chemical Engineering and Materials Science, University of California, Davis, CA 95616, USA
[b] Department Chemie und Biochemie, Physikalische Chemie, LMU München, Butenandtstrasse 5-13 (Haus E), 81377 München, Germany
[c] Institute of General and Inorganic Chemistry, Bulgarian Academy of Sciences, Sofia 1113, Bulgaria

ARTICLE INFO

Article history:
Received 27 August 2008
Revised 31 October 2008
Accepted 4 November 2008
Available online 9 December 2008

Keywords:
Gold catalyst
MgO
IR
CO oxidation
Deactivation
Carbonate
X-ray absorption spectroscopy

ABSTRACT

MgO-supported gold prepared by adsorption of $Au(CH_3)_2(acac)$ (acac is acetylacetonate) on partially dehydroxylated MgO was activated for CO oxidation catalysis by treatment in flowing helium at 473 K. X-ray absorption spectra showed that the activation involved reduction of the gold and formation of clusters (with an average diameter <10 Å) in which the gold was essentially zerovalent. During CO oxidation catalysis in a batch reactor, at least some of the gold was oxidized, as evidenced by the appearance of an $Au^{\delta+}$–CO band at 2151 cm^{-1} in the infrared (IR) spectrum. During operation in a flow reactor, the catalyst underwent deactivation, accumulating species such as carbonate and bicarbonate on its surface, as indicated by IR spectra. The accumulation of such species on the MgO support took place only during the initial period of operation of the catalyst, whereas the accumulation of such species on the gold continued throughout the operation, consistent with the inference that these species blocked catalytically active sites on the gold. The catalyst was reactivated by decomposition of these species by treatment in helium at 473 K. After three activation–deactivation cycles, the average diameter of the supported gold clusters had increased to about 30 Å, and the catalytic activity increased. Thus, the results provide a resolution of the separate effects on the catalytic activity of gold aggregation and accumulation of species such as carbonates and bicarbonates.

1. Introduction

Samples consisting of gold dispersed on metal oxide supports have been investigated extensively as catalysts for CO oxidation, motivated in large measure by Haruta's discovery [1] that some of these catalysts are highly active, even at temperatures much less than room temperature. Notwithstanding the extensive research, there are still many questions about the nature of the catalytically active sites, the reaction mechanisms, and catalyst deactivation.

The performance of these catalysts is sensitive to the support [2], the catalyst pretreatment conditions [3], the water content of the reactant mixture [4], and components such as chloride, which is present in commonly used precursors such as $HAuCl_4$ [5]. There is a lack of quantitative results characterizing the performance of supported gold catalysts, which is complicated by the catalyst deactivation.

Deactivation of supported gold CO oxidation catalysts has been ascribed variously to reduction and aggregation of the gold [6,7], other morphological changes in gold clusters [8], and reduction of the support surface [9]. The most commonly suggested causes of deactivation are sintering of gold clusters [10] and accumulation of carbonate-like species [4,11–13] (carbonates, bicarbonates, carboxylates, and formates). IR spectra of these species on catalyst surfaces are characterized by bands in the 1800–900 cm^{-1} region, including bands representing $\nu_{asym}(OCO)$, $\nu_{sym}(OCO)$, etc. [14].

These deactivation processes may occur simultaneously. For example, Konova et al. [15,16] found evidence of carbonate accumulation and gold agglomeration during CO oxidation catalyzed by Au/ZrO_2 and Au/TiO_2, observing that the two processes had different effects: sintering of gold caused irreversible deactivation (but the effect was usually small, with most supported gold catalysts retaining their activities as long as the average gold cluster diameter remained within a range of, typically, 2–5 nm); the accumulation of carbonate-like species, on the other hand, may lead to significant activity loss by blocking of active sites, although the effect can be reversed by removal of these species by treatment in inert gas at temperatures up to 573 K.

Deactivation caused by carbonate-like species can also be reversed by other treatments, such as addition of moisture. Kung et al. [17,18] investigated the roles of moisture and of H_2 on Au/Al_2O_3 catalysts, finding that both were effective in converting carbonate species to reactive formate species (which the authors proposed to be reaction intermediates), with regeneration of the catalyst. Daté

* Corresponding author.
E-mail address: bcgates@ucdavis.edu (B.C. Gates).

0021-9517/$ – see front matter
doi:10.1016/j.jcat.2008.11.005

et al. [4,13] drew a similar conclusion regarding the effect of moisture on Au/Al_2O_3 and Au/TiO_2.

Evidence of build-up of carbonate-like species on catalyst surfaces has emerged from infrared (IR) spectroscopy. The most informative spectra are those characterizing working catalysts, as they may provide correlations between carbonate accumulation and catalytic activity. For example, Shubert et al. [19] claimed that IR spectra gave evidence of carbonate and carboxylate ($-COO^-$) species during preferential oxidation of CO in a H_2-containing atmosphere catalyzed by Au/α-Fe_2O_3. As the amounts of these surface species increased with time on stream, the authors inferred that they were responsible for the deactivation. Similarly, Daté et al. [13] observed bands in the carbonate region (at 1435 and 1230 cm^{-1}) during CO oxidation catalyzed by Au/Al_2O_3. The change in intensity of the 1230-cm^{-1} band with time-on-stream correlated inversely with a measure of the catalytic activity for CO_2 formation. When moisture was introduced into feed stream, both bands decreased in intensity and disappeared, and the catalytic activity increased, leading the authors to suggest that carbonate-like species near the active sites caused deactivation.

In work with Au/CeO_2 [20], accumulation of carbonate-like species was indicated by IR bands at 1590, 1440, 1358, and 1270 cm^{-1}. The authors [20] inferred that some of these species were on the support and not the gold—and thus not responsible for the activity loss—whereas the monodentate carbonate species (characterized by the 1358-cm^{-1} band), formed on the support in a reaction with hydroxyl groups and bicarbonate species, did cause deactivation.

To develop a better understanding of the roles of carbonate-like species on supported gold catalysts, especially when the supports are strongly basic and readily form such species from CO and from CO_2 [14,21], our goal was to assess where the species form and whether their formation is influenced by gold. Specifically, we sought to distinguish carbonate-like species on gold and on a strongly basic support; to determine their effects on catalyst performance; and to distinguish the role of these species from that of aggregation of the gold. Thus, we investigated the adsorption of CO and of CO_2 separately on a basic support (MgO) and on Au/MgO. We report characterization of the surface species by IR spectroscopy and simultaneous measurements of the catalytic activity for CO oxidation, as well as characterization of fresh and used catalysts by extended X-ray absorption fine structure (EXAFS) spectroscopy to determine average gold cluster sizes, and by X-ray absorption near edge structure (XANES) spectroscopy to determine gold oxidation state(s). The results provide a basis for separating the effects of the formation of carbonate-like species, cluster growth, and modification of gold oxidation state(s) in the catalyst deactivation; the data demonstrate a correlation between carbonate-like species on gold and catalyst activity loss.

2. Experimental methods

2.1. Materials

He (Airgas, 99.995%) and CO (Airgas, 10% mixture balanced in He, 99.999%) were purified by passage through traps containing reduced Cu/Al_2O_3 and activated zeolite 4A to remove traces of O_2 and moisture, respectively. O_2 (Airgas, 10% in He, 99.999%) was purified by passage through a trap containing activated zeolite 4A to remove traces of moisture. The MgO support (EM Science, 97%, 60 m^2/g) was calcined in O_2 at 673 K for 2 h, followed by evacuation at 673 K for 16 h (pressure $< 10^{-2}$ Pa), and stored in an argon-filled glove box until it was used. *n*-Pentane solvent (Fisher, 99%) was dried and purified by refluxing over sodium metal and deoxygenated by sparging of N_2. The catalyst precursor $Au(CH_3)_2(acac)$ (acac = acetylacetonate, $C_5H_7O_2$) (Strem, 98%, handled as light- and temperature-sensitive) was used as supplied.

2.2. Catalyst preparation

The synthesis and handling of MgO-supported gold samples were carried out with exclusion of air and moisture on a double-manifold Schlenk vacuum line and in the glove box. Samples were prepared by slurrying $Au(CH_3)_2(acac)$ in dried and deoxygenated *n*-pentane with MgO at 298 K and 10^5 Pa. The slurry was stirred for 1 day, and the solvent was removed by evacuation for 1 day (pressure $< 10^{-2}$ Pa), giving a sample containing 1.0 wt% Au. The sample was stored in the glove box until used; part of it was sealed under vacuum in glass ampoules for transfer from California to Munich, where IR spectroscopy experiments were carried out in a batch system.

2.3. CO oxidation catalysis and product analysis by mass spectrometry

The as-prepared sample consisting of mononuclear Au(III) complexes bonded to the support [22] was tested at 303 K and atmospheric pressure for CO oxidation catalysis, either with or without pretreatment. The sample (typically, 0.10 g) was loaded into a once-through plug-flow reactor in the glove box and transferred to a flow system without coming in contact with air. In some experiments, the sample was tested for CO oxidation catalysis directly, with the partial pressures of the components in the reactant stream (Pa) being $P_{CO} = 1520$, $P_{O_2} = 1520$, and $P_{He} = 9.83 \times 10^4$. In other experiments, the sample was first treated in flowing helium at 473 K for 4 h and then cooled to 303 K in flowing helium to start the reaction, with the component partial pressures (Pa) being $P_{CO} = 510$, $P_{O_2} = 510$, and $P_{He} = 1.00 \times 10^5$. In the latter experiments (a test of the stability of the catalyst), the cycle of treatment in helium at 473 K followed by CO oxidation catalysis was repeated twice.

During treatment in flowing helium at 473 K and during CO oxidation catalysis, the effluent gases from the reactor were analyzed by mass spectrometry. The on-line instrument was a Balzers OmniStar running in multi-ion monitoring mode. Signals were recorded for the main fragments of CO ($m/e = 28$); O_2 ($m/e = 32$); CO_2 ($m/e = 44$); CH_4 ($m/e = 12, 15, 16$); C_2H_4 ($m/e = 27, 28$); and C_2H_6 ($m/e = 29, 30$). Signals are reported relative to that of the helium carrier gas ($m/e = 4$) to remove effects of small pressure fluctuations during the experiments.

2.4. Temperature-programmed decomposition (TPD)

TPD of the as-prepared sample consisting of mononuclear Au(III) complexes bonded to MgO [22] was carried out in a once-through plug-flow reactor. Helium flowed through the reactor as the temperature was increased from room temperature to 673 K at a rate of 3 K/min. An on-line gas chromatograph (Hewlett-Packard, HP-5890 series II) equipped with a 30-m × 0.53-mm DB-624 (J & W Scientific) capillary column (with N_2 as the carrier gas) and a flame-ionization detector was used to analyze the effluent gases.

2.5. X-ray absorption spectroscopy

Characterization of catalyst samples by X-ray absorption spectroscopy was carried out at beam line X-18B at the National Synchrotron Light Source (NSLS) at Brookhaven National Laboratory (BNL), Upton, NY, and at beam line 10-2 at the Stanford Synchrotron Radiation Laboratory (SSRL) of the Stanford Linear Accelerator Center (SLAC), Menlo Park, CA. The storage ring electron energy was 2.8 GeV at NSLS and 3 GeV at SSRL; the ring current varied within the ranges of 140–300 mA at NSLS and 50–100 mA at SSRL.

Powder samples were pressed into self-supporting wafers and mounted in a cell that allowed data collection under vacuum (pressure $< 1.33 \times 10^{-3}$ Pa) and at liquid nitrogen temperature. Sample masses were chosen to give an absorbance of 2.5 at the Au L_{III} edge (11919 eV). Each sample was scanned in transmission mode, with each spectrum being an average of 4 scans. To obtain a proper energy calibration, a gold foil was scanned simultaneously with each sample.

2.6. IR characterization of functioning catalysts

Transmission IR spectra of the calcined MgO support and of the as-prepared Au/MgO sample were recorded with a Bruker IFS 66v spectrometer operated with a spectral resolution of 4 cm^{-1}; each reported spectrum is an average of 16 scans. Samples were pressed into self-supporting wafers and loaded into a cell (In-situ Research Instruments, Inc., South Bend, IN) in the glove box. The cell allowed recording of spectra as treatment gases flowed through and around the wafer at temperatures ranging from room temperature to 573 K.

Blank IR experiments characterizing the species formed by exposure of the calcined MgO support alone to CO or CO_2 were carried out at room temperature. In the experiments characterizing the as-prepared Au/MgO, the sample in flowing helium was first treated at 473 K for 15 min and then cooled to 303 K. IR measurements were then carried out during CO oxidation catalysis with the sample at 303 K; the total feed flow rate was 100 mL (NTP) min^{-1} with CO and O_2 partial pressures of 510 Pa each (and the remainder helium).

2.7. IR characterization of catalysts in a batch system

IR spectra of the catalyst in a batch system were recorded in Munich. The IR cell permitted recording of spectra at temperatures between 85 K and ambient temperature [23]. The cell was connected to a vacuum adsorption system with a residual pressure $<10^{-3}$ Pa. Spectra were recorded with a Bruker IFS-66 spectrometer with a spectral resolution of 2 cm^{-1}; each reported spectrum is the average of 128 scans.

Sample powders were pressed into self-supporting wafers and then transferred to the IR cell in an argon-purged glove bag with the exclusion of air and moisture. The samples were subjected to various treatments in the cell, as described below. CO (>99.997%) used in these experiments was supplied by Linde AG; before use, it was further purified by passage through an Oxisorb cartridge. CO_2 (99.995%) was supplied by Messer-Griesheim GmbH.

3. EXAFS data analysis

Analysis of the EXAFS data recorded at the Au L_{III} edge was carried out with a difference file technique by use of the software XDAP [24]. The number of parameters used in fitting the data was justified statistically by the Nyquist theorem: $n = (2\Delta k \Delta r/\pi) + 1$, where Δk and Δr, respectively, are the ranges in k and r used in the data fitting (k is the photoelectron wave vector; r is the distance from the absorber Au atom) [25]. Criteria used to judge the appropriateness of a model tested in the data fitting were that both the magnitude and imaginary part of the Fourier-transformed data fit well with both k^1 and k^3 weightings of the data.

The models considered in the fitting included Au–Au contributions (both first- and second-shell contributions) and Au–support contributions (Au–O and Au–Mg). Amplitude- and phase-shift functions characteristic of the various EXAFS contributions were obtained either experimentally or from theoretical calculations by use of the software FEFF [26] (Supplemental Information). The amplitude reduction factor [27] was determined to be 0.92 by fitting the spectrum of gold foil by using the FEFF-generated reference for gold metal; this value was used in the analyses of the spectra of the supported samples. Fit diagnostic parameters characterizing the EXAFS models are presented in Supplemental Information.

4. Results

4.1. Activity of Au/MgO catalyst for CO oxidation

Results of earlier work [22] showed that the as-prepared Au/MgO sample contained mainly site-isolated, mononuclear Au(III) complexes having a structure analogous to that of the precursor $Au(CH_3)_2(acac)$, with the support surface being a bidentate ligand. The literature [28] indicates that the gold in these samples readily undergoes reduction and aggregation.

The activity of this sample was tested for CO oxidation catalysis at 303 K and atmospheric pressure, with a total feed flow rate of 100 mL (NTP) min^{-1} and CO and O_2 partial pressures of 1520 Pa each (with the remainder being helium). No CO_2 formation was detected after 1 h on stream by mass spectrometry; the catalyst had negligible activity for CO oxidation under these conditions.

The activity of the catalyst became evident after activation in flowing helium at 473 K for 4 h. The process, which can be described as a temperature-programmed decomposition, was followed by mass spectrometric analysis of the gas-phase products. No effluent gases other than helium were detected at temperatures up to 423 K, but at higher temperatures, evolution of fragments with $m/e = 15, 28, 29$, and 30 was recorded, suggesting the formation of a mixture of hydrocarbons (Fig. 1). Analysis of the effluents by gas chromatography indicated methane, ethane, and ethylene (data not shown). Thus, we infer that the original mononuclear gold species bonded to MgO decomposed during the heating as the methyl ligands on gold underwent reaction [29].

After cooling of the activated Au/MgO sample to 303 K in flowing helium, the flow of CO and O_2 started, and the catalyst performance for CO oxidation was tested. CO_2 was the only product detected.

Like many supported gold catalysts, ours deactivated rapidly, reaching a near-steady-state conversion after about 600 min on stream (Fig. 2A).

Treatment in flowing helium at 473 K for 4 h reactivated the catalyst (Fig. 2A). During the reactivation, CO_2 was released from the catalyst, as indicated by mass spectrometry data showing an intensity change of the $m/e = 44$ fragment (Fig. 2B). The activation–deactivation cycle was repeated twice. After each activation process, the catalyst showed deactivation behavior similar to that mentioned before (Fig. 2A). However, the initial and near-steady-state conversions increased from one cycle to the next: from the first to the second cycle, this conversion increased from 1.7 to 2.8%; after the third cycle, it had increased to 3.6%.

4.2. XANES and EXAFS characterizations of Au/MgO

4.2.1. Characterization of the catalyst after treatment in helium

When the as-prepared Au/MgO sample was treated in helium at 473 K, its color changed from white to purple, consistent with the formation of zerovalent gold clusters on the support [30,31]. To provide evidence of the oxidation state of gold and the average diameter of the gold clusters, the catalysts were characterized by XANES and EXAFS spectroscopies, respectively.

XANES at the Au L_{III} edge provides qualitative information about the oxidation state of gold. XANES peak locations and intensities characterizing reference compounds with gold in various oxidation states, summarized elsewhere [32,33], provide a partial basis for interpreting the data. The spectrum of Au/MgO treated in

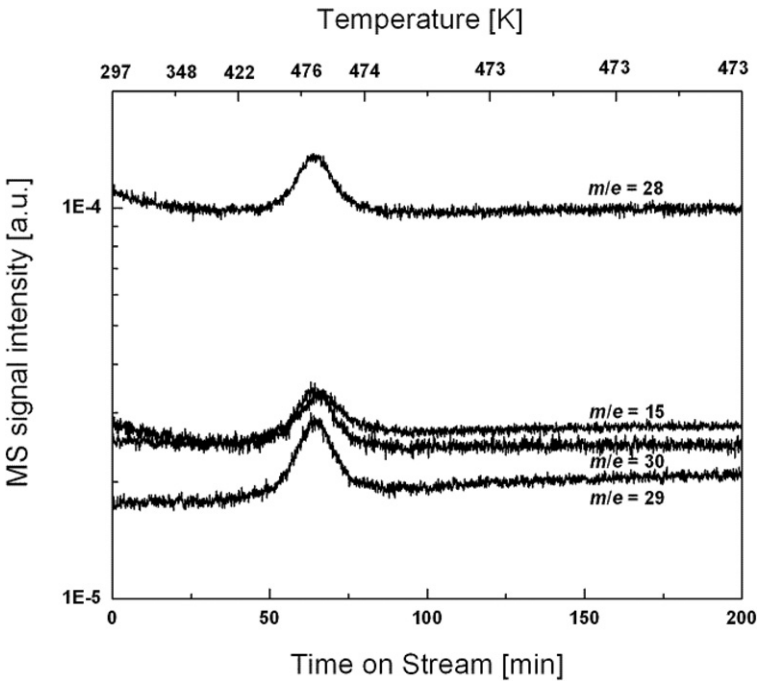

Fig. 1. Changes in intensity of the mass spectral signals of the effluent gases from the flow reactor when the sample made by bringing $Au(CH_3)_2(acac)$ in contact with partially dehydroxylated MgO was treated in flowing helium as the temperature was increased.

helium at 473 K for 4 h (Fig. 3, spectrum a) is characterized by features similar to those of gold foil, including the lack of an absorption peak at about 4 eV above the absorption edge. This result is a strong indication that most of the gold in the sample was zerovalent.

Analysis of the EXAFS data characterizing this sample gave evidence of Au–Au and Au–O contributions; the parameters determined in the fitting are shown in Table 1. A model containing only a first-shell Au–Au contribution did not give a satisfactory fit of the data (details are given in Supplemental Information). However, a good overall fit was obtained when two Au–Au shells were included.

Two first-shell Au–Au contributions are characterized by distances of 2.79 Å (with a coordination number of 2.5) and 2.87 Å (with a coordination number of 4.9) (Supplemental Information). A small Au–O contribution (with a coordination number of 0.5) was detected at 2.15 Å. The Au–Au coordination number of 2.5 corresponds to clusters with approximately 4 Au atoms each, on average, and the coordination number of 4.9 to clusters with approximately 12 Au atoms each, on average, and an average diameter less than 10 Å.

4.2.2. Characterization of the catalyst after activation–deactivation cycles

To understand the stability of the treated Au/MgO sample, we also characterized it after three activation–deactivation cycles equivalent to those described above. As expected, the XANES spectrum of the used catalyst (Fig. 3, spectrum b) is similar to that of the helium-treated Au/MgO sample before the catalytic reaction (Fig. 3, spectrum a), giving evidence of zerovalent gold. Consistent with the XANES data, the EXAFS data indicate an Au–Au contribution (Supplemental Information), showing that the sample contained gold clusters; the coordination number was found to be 10 with a distance of 2.84 Å (Table 1).

Thus, the data show that an increase in the average gold cluster size resulted from the treatment in helium and also from the exposure to CO and O_2 during catalysis: the first-shell Au–Au coordination number of 10 corresponds to clusters of roughly 800 Au atoms each, on average (according to the model of Jentys [34]); if these clusters are assumed to be spherical, their average diameter is calculated to be about 30 Å [34].

4.3. IR characterization of Au/MgO during treatment in helium at 473 K

IR characterization was carried out during treatment of the as-prepared Au/MgO in flowing helium at 473 K to further understand the structural changes that took place in the activation process. The spectra (Figs. 4A and 4B) show that as the temperature increased to >437 K, there were marked decreases in intensity of the C–H stretching bands (at 2956, 2906, and 2821 cm^{-1}; Fig. 4A, spectra e and f). These C–H stretching bands arise from methyl ligands bonded to gold and from acac ligands bonded to MgO [28]. The IR results are thus consistent with the mass spectrometry data showing the reaction of the methyl ligands on gold at temperatures >423 K (Fig. 1). Simultaneously, slight decreases in the intensities of the bands in the 1800–1000 cm^{-1} region (attributed to acac ligands) were observed at temperatures >437 K (Fig. 4B, spectra e and f). The spectra shown in Figs. 4A and 4B indicate that, at 473 K, most of the methyl ligands had been removed from the gold, although considerable amounts of acac or species formed from acac were evidently still bonded to the MgO.

The IR data are consistent with the XANES and EXAFS results, as follows: The presence of the methyl groups on gold in the initially prepared sample is indicated by the EXAFS data, specifically, the Au–C contribution with a coordination number of 2 at a distance of 2.04 Å [22]. The XANES data indicate a gold oxidation state of approximately +3 characterizing this sample, as in the precursor [22].

After treatment of the sample in helium at 473 K, it was no longer characterized by detectable Au–C contributions, as indicated by the EXAFS data of Table 1; this observation is also consistent with the IR results stated in the preceding paragraph. Instead, two first-shell Au–Au contributions were observed (Table 1), indicating that clusters formed when the methyl groups were removed. After formation of the clusters, the oxidation state of gold was indicated by XANES to be essentially 0 (Fig. 3, spectrum a).

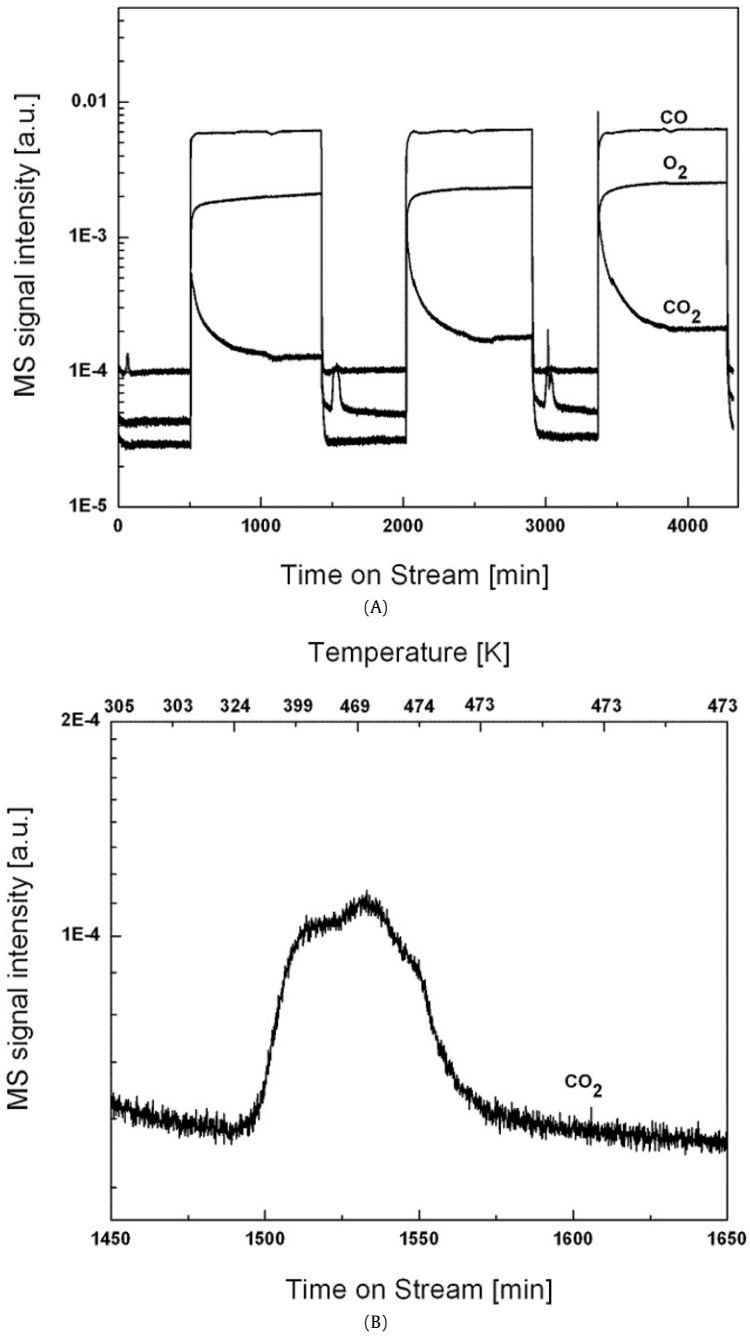

Fig. 2. (A) Changes in intensity of the mass spectral signals of the effluent gases from the flow reactor containing the sample made by bringing $Au(CH_3)_2(acac)$ in contact with partially dehydroxylated MgO as it went through treatment at 473 K for 4 h in flowing helium followed by CO oxidation at 303 K for 15 h; the cycle was repeated twice. (B) Changes in intensity of the mass spectral signal for CO_2 in the effluent gas from the flow reactor when the Au/MgO sample after 20 h of continuous operation as a CO oxidation catalyst was treated in flowing helium as the temperature was increased.

In summary, the IR, EXAFS, and XANES data confirm that the Au/MgO sample treated in flowing helium at 473 K contained gold clusters that can be well approximated as zerovalent and from which the initially present methyl ligands had been removed.

4.4. IR characterization of MgO and Au/MgO during exposure to CO and to CO_2

4.4.1. Exposure of MgO to CO and to CO_2

During CO oxidation catalyzed by Au/MgO in the flow reactor, surface carbonate-like species might be expected to form from reactant CO and/or from product CO_2. To distinguish IR bands characteristic of species bonded to gold and those bonded to the MgO support, we first treated the MgO alone with CO and with CO_2.

Interpretation of the spectra is based on a number of literature reports investigating the adsorption of CO and of CO_2 on MgO [35–42], as follows. At low temperatures, CO adsorption leads to the appearance of complex spectra, because of the formation of carbonyls and negatively charged monomeric, dimeric, and polymeric species [36–38]. In these cases, bands at approximately 2100 cm^{-1} always appear in the carbonyl stretching region. Adsorption of CO_2 on MgO results in the formation of various carbonate-like structures, and the relative concentrations of these species depend on the sample morphology and the experimental conditions [39–41].

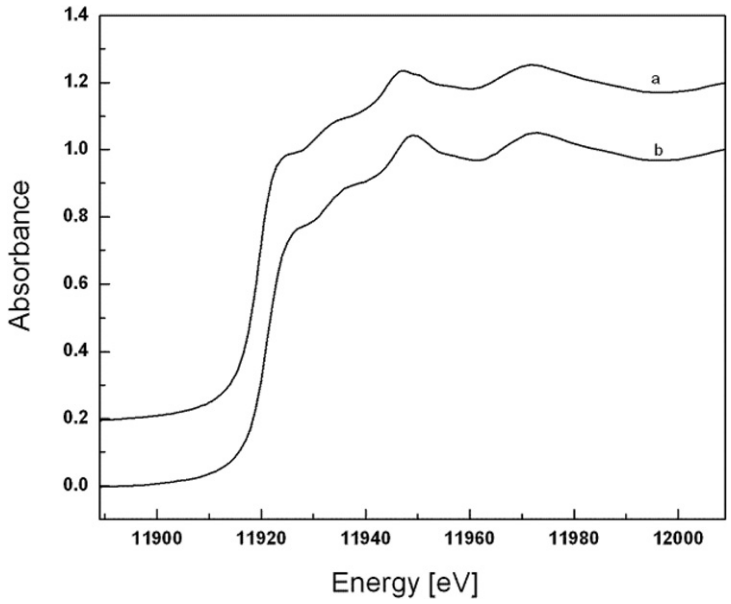

Fig. 3. XANES spectra of (a) the Au/MgO sample made by bringing $Au(CH_3)_2(acac)$ in contact with partially dehydroxylated MgO treated in flowing helium at 473 K for 4 h; (b) the Au/MgO sample made by bringing $Au(CH_3)_2(acac)$ in contact with partially dehydroxylated MgO after it went through treatment at 473 K for 4 h in flowing helium followed by CO oxidation at 303 K for 15 h; the cycle was repeated twice.

Table 1
EXAFS results at the Au L_{III} edge characterizing MgO-supported gold species formed by treatment in flowing helium at 473 K of species formed by adsorption of $Au(CH_3)_2(acac)$ on MgO (a) before CO oxidation catalysis ($\Delta k = 3.38$–14.95 Å^{-1}, $\Delta r = 1$–4.5 Å); and (b) after three cycles of CO oxidation catalysis followed by catalyst reactivation ($\Delta k = 3.43$–15.03 Å^{-1}, $\Delta r = 1$–4.5 Å).

Sample	Shell	N	R (Å)	$10^3 \times \Delta\sigma^2$ (Å^2)	ΔE_0 (eV)
Before CO oxidation reaction	Au–O	0.5	2.15	1.0	−7.7
	Au–Au (1)	2.5	2.79	2.9	−4.4
	Au–Au (2)	4.9	2.87	3.6	−4.4
	Au–Au (3)	1.4	4.05	4.7	−4.4
	Au–Mg	0.7	4.23	0.0	−2.2
After three cycles of CO oxidation	Au–Au (1)	10.0	2.84	6.3	−5.0
	Au–O[a]	0.3	3.17	−8.5	−6.0
	Au–Au (2)	2.4	4.07	1.5	−5.0
	Au–Mg	1.1	4.15	4.4	2.3

Notation: N, coordination number; R, distance between absorber and backscatterer atoms; $\Delta\sigma^2$, relative Debye–Waller factor; ΔE_0, inner potential correction.
[a] This contribution is too small to allow a confident assignment. It was included to make the overall fitting complete.

Formation of carbonate-like species on partially dehydroxylated MgO during adsorption of CO and of CO_2 was investigated by Smart et al. [35]. Various unidentate species (characterized by IR bands at 1520 and 1390 cm^{-1}) and bidendate carbonate species (characterized by an IR band at 1670 cm^{-1}) were identified, as illustrated by structures A and B, respectively:

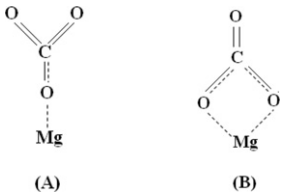

(A) (B)

Rethwisch and Dumesic [39], in an investigation of the coadsorption of CO and CO_2 on MgO, established the formation of unidentate and bidentate carbonates as well as bicarbonates. Consistent with the results of Smart et al. [35], the unidentate carbonates were characterized by ν_{as} bands at 1570–1518 cm^{-1} and ν_s bands at 1385–1310 cm^{-1}, whereas bands at 1735–1680 cm^{-1} and 1024 cm^{-1} were indicative of bidentate carbonates. The latter species were not observed after evacuation of the sample at 660 K. Furthermore, the bicarbonates were identified by a set of bands at 1638, 1440–1420, and 1210 cm^{-1}. Di Cosimo et al. [40] also demonstrated the formation of unidentate and bidentate carbonates, the latter species being characterized by bands at 1630–1610 cm^{-1} and 1340–1320 cm^{-1}. In contrast, Mekhemer et al. [41] found two types of unidentate carbonates (ν_{as} at ca. 1520 and 1500 cm^{-1} and ν_{as} at 1450 and 1405 cm^{-1}, respectively). These authors also detected bidentate carbonates (1690 and 1360–1320 cm^{-1}) and bicarbonate species (1646, 1405, and 1225 cm^{-1}).

When CO flowed into our IR cell containing the MgO wafer at room temperature, only gas-phase CO was detected in the C–O stretching region of the spectrum. However, several absorption bands in the 1800–900 cm^{-1} region grew in with time on stream (Fig. 5). Initially, weak bands developed at 1668, 1500, 1375, and 1217 cm^{-1} (Fig. 5, spectrum b). All these bands increased in intensity with time on stream (Fig. 5, spectrum c), and a shoulder at 1385 cm^{-1} became resolved within 15 min. A weak band at 1003 cm^{-1} was also discernible. Furthermore, shoulders at 1649, 1540, 1413, and 1340 cm^{-1} developed after approximately 30 min on stream. After 15 min on stream, the band at 1217 cm^{-1} started to decrease in intensity. Difference spectra show that components at 1668, 1375, and 3626 cm^{-1} decreased in concert with this band (inset, Fig. 5).

On the basis of literature data [35,39–41,43,44] and the analysis of the difference spectra, we assign the broad bands at about 1500 and 1385 cm^{-1} to the split ν_3 vibration of unidentate carbonate species on MgO. The corresponding ν_1 mode is IR inactive for the free carbonate ion, but it appeared in our spectra with a low intensity (at 1003 cm^{-1}) as a result of the lowered symmetry. These species form relatively quickly on the surface.

Two other kinds of unidentate carbonates were also observed, with lower concentrations. One of them, characterized by a set of bands at approximately 1520 and 1340 cm^{-1}, continuously rose in concentration, and another, characterized by bands at 1540 and 1413 cm^{-1}, formed predominantly at the end of the experiment. A set of bands at 3626, 1668, 1375, and 1217 cm^{-1} is assigned to bicarbonates.

Furthermore, two bands formed, at 1645 and 1400 cm^{-1}, that are indicative of bidentate carbonates. These species were formed

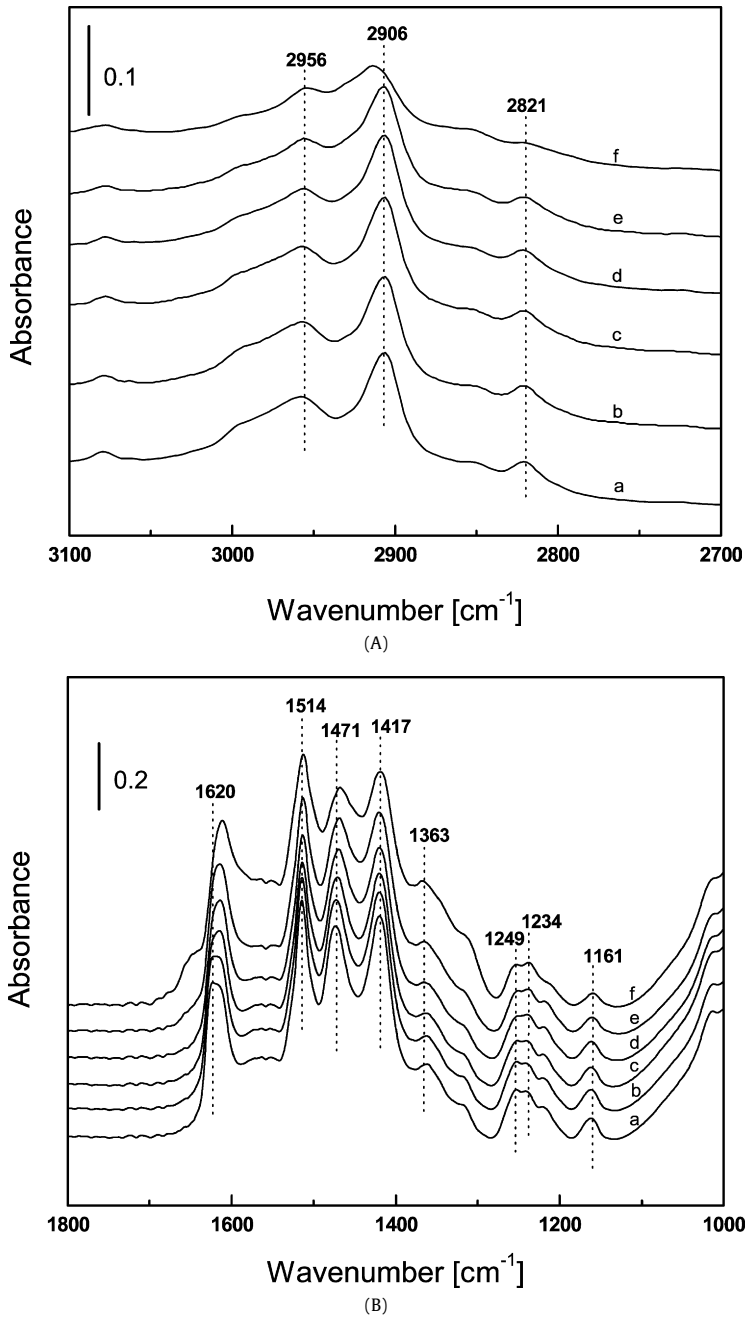

Fig. 4. Changes in the IR spectra in the (A) 3100–2700 cm^{-1} region and (B) 1800–1000 cm^{-1} region when the sample made by bringing $Au(CH_3)_2(acac)$ in contact with partially dehydroxylated MgO was treated in flowing helium at increasing temperatures (K): (a) 304; (b) 326; (c) 357; (d) 397; (e) 437; and (f) 473.

after 15 min on stream. Small deviations of the wavenumbers were observed depending on the coverage. We emphasize that no bands in the carbonyl and C–H stretching regions were detected, and this result excludes the formation of (i) carbonite-type and (ii) formate species.

When CO_2 was brought in contact with MgO, several IR bands appeared very fast in the 1800–900 cm^{-1} region (Fig. 5, spectrum h), similar to those observed during exposure of MgO to CO. The positions of these bands are slightly different from those of the bands characterizing the structures formed from CO and MgO, being observed at frequencies 5 or 6 cm^{-1} greater than those characterizing the latter. The overall intensity of the bands was greater than those observed in the CO adsorption experiments. In particular, bidentate carbonates (bands at 1649, 1400, and 1026 cm^{-1}) were formed at a much higher concentration. This result indicates that the formation of carbonate-like species when CO reacts with MgO is limited by some forms of reactive oxygen on the surface. Nonetheless, the results allow us to conclude that essentially the same carbonate-like species were formed on MgO during exposure to either CO or CO_2.

Treatment of the MgO with CO and with CO_2 led to marked changes in the IR spectra in the O–H stretching region (data not shown), including a decrease in intensity of the 3756-cm^{-1} band and the appearance of a sharp band at 3626 cm^{-1} (O–H stretching mode, already assigned to bicarbonates) and a broad band at 3476 cm^{-1}. The band at 3476 cm^{-1} has already been reported by Li et al. [42] for a carbonate-precovered MgO sample. These results suggest interactions between adsorbed carbonate-like species and surface hydroxyl groups through hydrogen bonding [35].

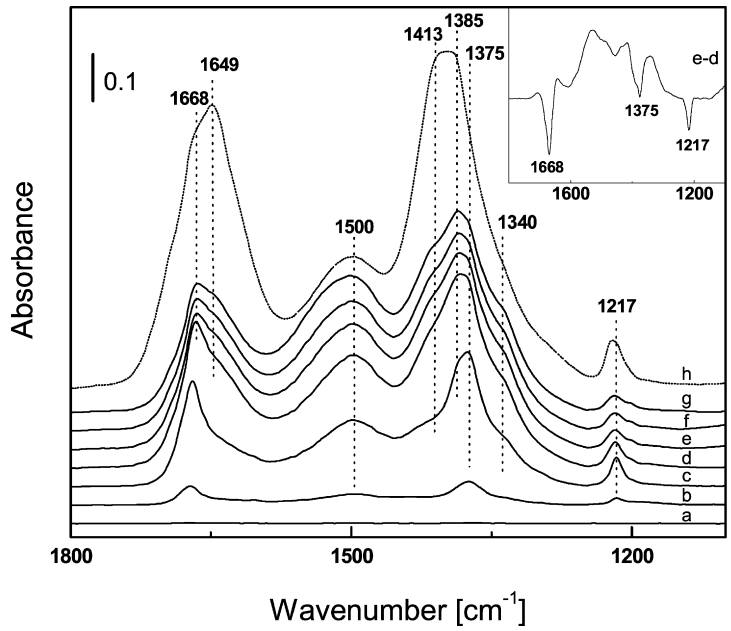

Fig. 5. IR difference spectra in the 1800–900 cm^{-1} region recorded during CO treatment of MgO (calcined at 673 K) at room temperature with increasing times on stream (min): (a) 0; (b) 3; (c) 15; (d) 30; (e) 45; (f) 60; and (g) 117. Spectrum h was recorded during a separate CO_2 treatment of MgO after 3 min.

4.4.2. Exposure of activated Au/MgO to CO and to CO_2

As a next step toward elucidation of the locations of the surface species formed from CO and from CO_2, the MgO was replaced by Au/MgO in the IR experiments. In contrast to the treatment of MgO alone, the treatment of the fresh, as-prepared Au/MgO first involved contacting of the sample with helium at 473 K for 15 min to remove the methyl ligands. The sample was then cooled in flowing helium to 303 K. CO or, in a separate experiment, CO_2 was then introduced into the IR cell, and spectra were recorded. All the bands characteristic of carbonate-like species on MgO alone were again observed with the sample in contact with either CO or CO_2, with small differences in the frequencies of some of them relative to those observed during exposure of MgO to CO or to CO_2. Moreover, some bands, such as those characterizing unidentate carbonates (1500 and approximately 1380 cm^{-1}), appeared with reduced intensity. This result might be taken as evidence of blocking of the magnesia surface by gold species, although the concentration of gold on the surface was low. The intensities of the bands grew in faster during CO_2 treatment than during CO treatment. However, the intensity of the CO–H deformation band at approximately 1217 cm^{-1}, after passing through a maximum, declined over time during exposure of the sample to CO_2 (similar to what was observed during exposure of MgO alone to CO); furthermore, several new bands appeared during treatment in CO, including bands at about 1606, 1566, 1534, 1300 and 1010 cm^{-1} (Fig. 6A). When CO_2 was brought in contact with the sample, the overall intensity of the bands attributed to carbonate-like species was higher, and in this case three components at lower frequencies, namely, at 1343, 1315, and 1277 cm^{-1}, became clearly discernible (Fig. 6B). Because these bands were observed only when gold was present on the MgO, they are assigned to three types of carbonates formed on gold. This assignment is central to the interpretation presented here and is considered further in Section 5.

In summary, exposure of Au/MgO treated in flowing helium at 473 K to either CO or CO_2 led to the formation of various carbonate-like species on the sample surface. By comparing IR spectra characterizing MgO (which had undergone no further treatment besides calcination at 673 K) and Au/MgO (treated in flowing helium at 473 K) after exposure to CO and, separately, to CO_2, we were able to differentiate the carbonate-like species formed on gold from those formed on MgO: the carbonate-like species on gold are characterized by IR bands at 1606, 1566, 1534, 1343, 1315, 1277 and 1010 cm^{-1}, whereas those on MgO are characterized by bands at approximately 1660, 1500, 1380, 1217, and 1003 cm^{-1}.

4.5. IR characterization of Au/MgO during CO oxidation catalysis

An Au/MgO sample was used to catalyze CO oxidation at 303 K after activation in flowing helium at 473 K for 15 min. IR spectra recorded during the catalytic reaction (Fig. 7) are characterized by absorption bands similar to those observed as CO and, separately, CO_2 were in contact with the Au/MgO sample treated similarly (Supplemental Information). The bands characteristic of various carbonate-like species on MgO (including those of bicarbonates at approximately 1660, 1380, and 1219 cm^{-1}) grew in within the first few minutes of the catalytic reaction in the flow system (Fig. 7). In contrast, the bands at 1604, 1569, 1531 and 1338 cm^{-1} grew in more slowly (Fig. 7); small increases in intensities were still being observed even after more than 600 min on stream.

The effluent gases from the IR cell (monitored by mass spectrometry) included CO_2, indicating catalytic oxidation of the CO. The catalyst lost activity with time on stream, as shown by the decrease in the intensity of the mass spectral signal $m/e = 44$, similar to what is shown in Fig. 2A.

To re-activate the Au/MgO after 20 h of continuous CO oxidation catalysis, the IR cell was purged, and the sample was treated in flowing helium at 473 K for 15 min. During this treatment, all the bands characteristic of surface carbonate-like species decreased in intensity (Supplemental Information), consistent with the concomitant release of CO_2 detected by mass spectrometry (Fig. 2B). The activity of the catalyst after this treatment had increased, and the behavior of the sample was similar to that shown in Fig. 2A.

4.6. IR characterization of Au/MgO during treatment in CO and during CO oxidation catalysis in a batch cell

The IR characterization of Au/MgO in the flow system provided information about the surface carbonate-like species formed during CO oxidation catalysis. However, bands characterizing surface gold carbonyl species could not be detected in these experiments,

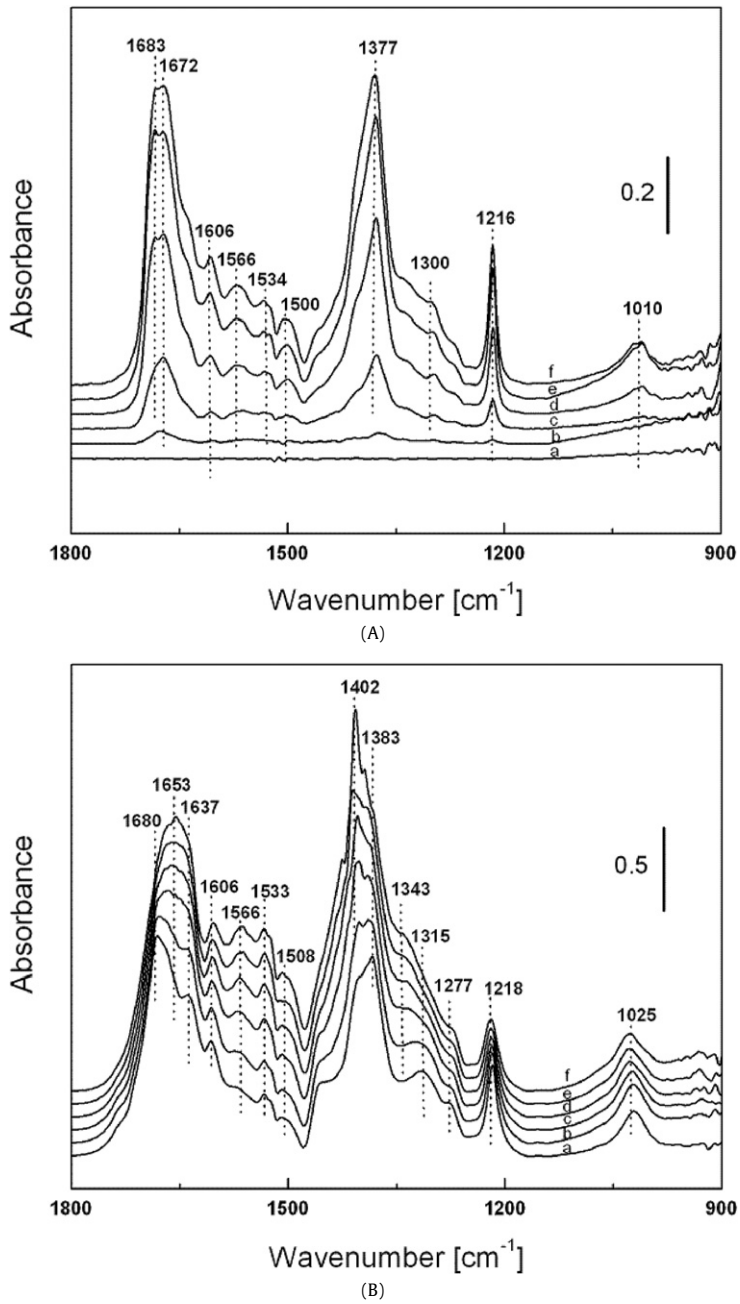

Fig. 6. IR difference spectra in the 1800–900 cm^{-1} region recorded during (A) CO and, separately (B), CO_2 treatment of Au/MgO made by bringing $Au(CH_3)_2(acac)$ in contact with partially dehydroxylated MgO (pretreated in helium at temperatures up to 473 K) at room temperature with increasing time on stream (min): (a) 0; (b) 3; (c) 15; (d) 30; (e) 45; and (f) 60.

because of their low intensities. Consequently, further IR experiments were carried out in Munich with a batch IR cell that provided more informative spectra [45].

4.6.1. Interaction of CO with Au/MgO

An Au/MgO sample was evacuated at various temperatures in the IR cell, and then the state of gold was tested by adsorption of CO at room temperature. When the sample was evacuated at temperatures below 373 K, no CO adsorption was observed (Supplemental Information; Fig. 7, spectra a–c). Because mass spectrometry results suggest that the mononuclear gold species decomposed only after the temperature had increased to >423 K, we propose that the lack of CO adsorption on gold is an indication that the gold sites were still fully coordinated.

In contrast, when CO was brought in contact with the sample activated under vacuum at 423 K, two weak carbonyl bands appeared, at 2128 and 2092 cm^{-1}, which are assigned to $Au^{\delta+}$–CO and Au^0–CO species, respectively [45]. When the temperature of evacuation was increased to 473 K, two carbonyl bands arose, at 2084 and 2038 cm^{-1} (Supplemental Information). The band at 2038 cm^{-1} was more resistant to removal by evacuation than the other. On the basis of earlier work [45], we assign the 2038-cm^{-1} band to $Au^{\delta-}$–CO species formed from gold anions located on gold clusters (possibly formed on defect sites [46,47]). The high stability of the species and the low frequency of the band are indicative of enhanced π-back donation favored by the negatively charged gold sites [45]. The band at 2084 cm^{-1} is assigned to Au^0–CO species, but we cannot rule out some partial negative charge on these sites.

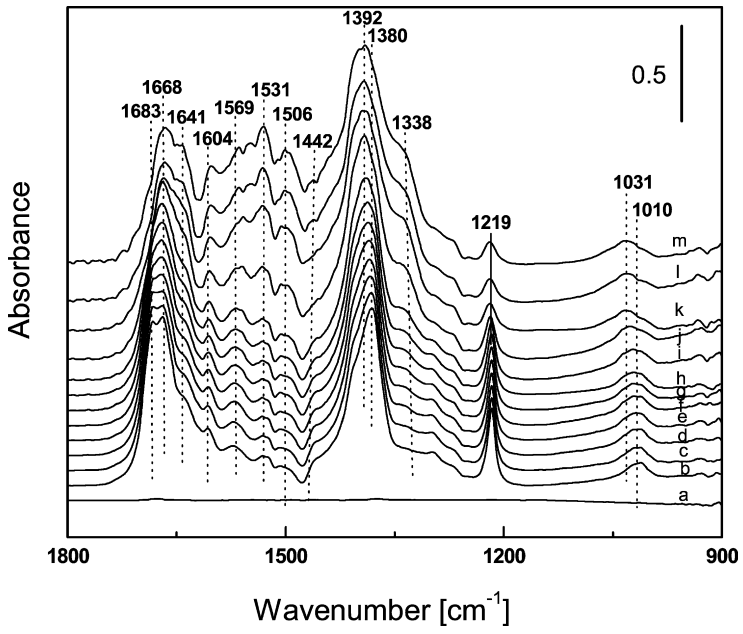

Fig. 7. IR difference spectra in the 1800–900 cm^{-1} region during CO oxidation at 303 K catalyzed by Au/MgO made by bringing $Au(CH_3)_2(acac)$ in contact with partially dehydroxylated MgO (pretreated in helium at temperature up to 473 K) with increasing time on stream (min): (a) 0; (b) 5; (c) 15; (d) 30; (e) 45; (f) 60; (g) 75; (h) 90; (i) 120; (j) 240; (k) 480; (l) 900; (m) 1200.

In summary, the results of these experiments show that, consistent with the XANES and EXAFS results, a temperature of 473 K was high enough to remove the methyl ligands and cause reduction of the gold on the MgO.

4.6.2. CO oxidation on Au/MgO

When the evacuated catalyst was exposed to a $CO + O_2$ mixture, the band at 2040 cm^{-1} almost disappeared; the band at 2084 cm^{-1} shifted to 2095 cm^{-1}; and a new band developed, at 2151 cm^{-1} (Fig. 8). The behavior of the bands in the range of 2084–2095 cm^{-1} essentially matches that of the comparable bands characterizing Au/La_2O_3 [48]. The development of the band at 2151 cm^{-1} suggests a high density of $Au^{\delta+}$ sites (these represent Au^+ ions on gold clusters). It has been reported [49] that such sites form from metallic gold only after severe oxidation. However, the results can be explained by the suggestion that the $Au^{\delta-}$ sites on the activated sample were present in a relatively high density and that, when oxidized by CO_2, were converted into $Au^{\delta+}$ sites [48].

Besides the CO adsorption bands, a band at 2345 cm^{-1} (adsorbed CO_2) and a series of bands at wavenumbers <1800 cm^{-1} grew in; these are attributed to carbonate-like species (data not shown). The positions of these bands are similar to those shown in Fig. 7.

4.6.3. Reoxidation of Au/MgO by O_2 and by CO_2

To clarify the nature of the oxidizing agent of gold during the catalytic CO oxidation reaction, we investigated the re-oxidation of gold by O_2 and by CO_2. Fig. 9 shows the spectra of Au/MgO after various treatments. When the reduced Au/MgO was treated with O_2 at room temperature, subsequent exposure to CO led to a spectrum (Fig. 9, spectrum b) essentially matching that recorded after exposure of a sample to CO prior to contacting with O_2. Therefore, we infer that O_2 alone was able to oxidize neither the Au^0 nor the $Au^{\delta-}$ sites.

When the catalyst was exposed to a mixture of $CO + O_2$, the band at 2042 cm^{-1} almost disappeared; the band at 2084 cm^{-1} shifted to 2095 cm^{-1}; and a new band developed, at 2151 cm^{-1} (Fig. 8, spectrum d; Fig. 9, spectrum c). Essentially the same spectrum was also recorded after CO adsorption on a sample of Au/MgO (activated by treatment under vacuum at 473 K) that after activation had been treated with CO_2 (2 kPa, 10 min, room temperature, followed by evacuation) (Fig. 9, spectrum d). The results demonstrate that CO_2 acted as an oxidizing agent of reduced gold sites (Au^0 and $Au^{\delta-}$), consistent with an earlier report [48].

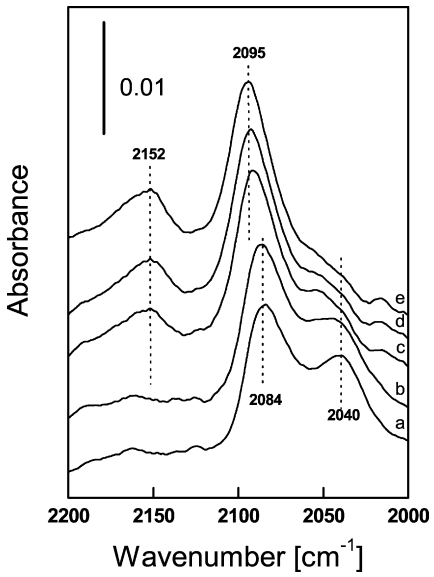

Fig. 8. IR spectra of CO (2 kPa equilibrium pressure) adsorbed at room temperature on Au/MgO made by bringing $Au(CH_3)_2(acac)$ in contact with partially dehydroxylated MgO (evacuated at 473 K): (a) before the introduction of O_2; after the subsequent introduction of O_2 (100 Pa partial pressure) at room temperature with increasing time (min): (b) 1, (c) 5, (d) 10, (e) 20. Spectra are background and gas-phase corrected and smoothed.

5. Discussion

5.1. Interactions of CO and of CO_2 with MgO

After adsorption of CO and CO_2 on the MgO sample we have established formation of surface uni- and bidentate carbonates as well as of bicarbonates. All these species were observed by various

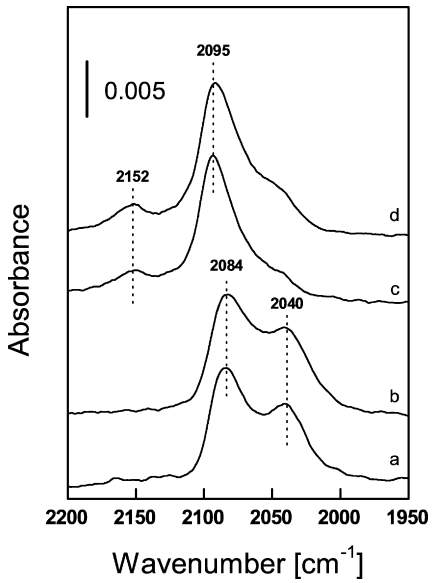

Fig. 9. IR spectra of CO (2 kPa equilibrium pressure) adsorbed at room temperature on Au/MgO made by bringing $Au(CH_3)_2(acac)$ in contact with partially dehydroxylated MgO (evacuated at 473 K before each experiment) after the following treatments: (a) just after evacuation at 473 K for 1 h; (b) introduction of O_2 (10 kPa, 20 min at room temperature, evacuation at room temperature); (c) coadsorption of CO and O_2 (2 and 0.1 kPa, 10 min at room temperature, evacuation at room temperature); (d) introduction of CO_2 (2 kPa, 10 min at room temperature, evacuation at room temperature). Spectra are background and gas-phase corrected and smoothed.

authors with other MgO preparations [35,39–41]. However, Smart et al. [35] and Di Cosimo et al. [40] did not observe bands near 1217 cm^{-1} during exposure of their samples to CO or CO_2.

Daté et al. [13] observed a band at 1230 cm^{-1} during CO_2 adsorption on Al_2O_3, which they inferred to originate from carbonate-like species. Manzoli et al. [50] observed a band at 1226 cm^{-1} during CO oxidation catalysis on Au/ZnO, which they ascribed to a bending mode of OH groups in surface bicarbonates. Henao et al. [51] detected a band at 1242 cm^{-1} during CO adsorption on Au/TiO_2 and assigned it to a surface hydroxycarbonyl (they found that the band disappeared when the sample was exposed to O_2).

We exclude the last of these assignments, because, in our case, the 1217-cm^{-1} band was also observed during exposure of the sample to CO_2. As was already stated, the simultaneous appearance of a band at 3626 cm^{-1} indicates that the assignment to bicarbonate species is the most compelling. In some experiments we observed that the band at 1217 cm^{-1} passed through a maximum with time on stream, an observation that suggests the spontaneous decomposition of bicarbonates. However, we emphasize that the various behaviors of this band during the sample treatments in CO and CO_2 are still not understood fully. Although it is only speculative, we might infer a reaction of a bicarbonate species with an OH group to form a carbonate and water.

Hydroxyl groups on the MgO play an important role during adsorption of both CO and CO_2, as evidenced by the changes in the O–H stretching region of the IR spectra (data not shown). Interactions between surface hydroxyl groups and carbonate-like species, as well as accurate assignments of the adsorption bands in the 1800–1000 cm^{-1} region, were discussed further by Smart et al. [35].

5.2. Activation of Au/MgO for CO oxidation catalysis

Unlike the sample similarly prepared by bringing $Au(CH_3)_2(acac)$ in contact with zeolite NaY [6], the as-prepared Au/MgO sample containing site-isolated, mononuclear Au(III) species did not have detectable activity for CO oxidation at room temperature. This difference seemingly cannot be explained by a support effect alone, as both supports are irreducible and have not been found to activate O_2. The different catalytic behaviors may instead arise from differences in the stability of the mononuclear gold species on the two supports. When $Au(CH_3)_2(acac)$ was adsorbed to form mononuclear complexes on zeolite NaY, methyl ligands could be removed easily from the gold, and IR bands characteristic of CO adsorbed on gold could be detected even with the sample evacuated at room temperature [6,52]. However, when the support was MgO, methyl ligands were more stably bonded to the gold, and the gold was evidently coordinatively saturated at room temperature—no CO adsorption on gold was observed by IR spectroscopy.

To activate the Au/MgO sample for CO oxidation catalysis, the methyl ligands on gold had to be removed—by treatment in helium at temperatures exceeding 423 K, as evidenced by both mass spectrometry (Fig. 1) and IR (Fig. 4A) results. XANES (Fig. 3) and EXAFS data (Table 1) show that removal of the methyl ligands was accompanied by reduction and aggregation of the gold, as expected [29].

5.3. Active gold species for CO oxidation catalysis

The EXAFS and XANES data respectively indicate that the activated Au/MgO catalyst contained gold clusters and that these were principally zerovalent gold. Therefore, it might seem to be appropriate to infer that zerovalent gold clusters are active for CO oxidation catalysis, consistent with the reasoning of numerous authors [53,54].

IR characterizations of the catalyst under CO oxidation conditions provide further insight into the nature of the gold species: as for the Au/La_2O_3 sample investigated before [48], CO_2 oxidized Au^0 in supported clusters to form some $Au^{\delta+}$ sites. As a result, the Au/MgO sample is inferred to have contained mixtures of Au^0 and $Au^{\delta+}$ species under catalytic reaction conditions. We infer that one or both of these species might be involved in the catalytic reaction, and we speculate that the active gold species might contain both, perhaps with the charged species being at the metal–support interface [55,56].

5.4. Deactivation of Au/MgO during CO oxidation catalysis

Numerous researchers have used IR spectroscopy to investigate the accumulation of carbonate-like species on supported gold catalysts during CO oxidation. However, as a consequence of the formation of more than one kind of carbonate-like species and the lack of blank experiments with the supports alone, it has been difficult to distinguish the species formed on the support, at the gold–support interface, and on the gold—and thus it has not been a straightforward matter to determine the cause(s) of deactivation.

Konova et al. [15] proposed that on their Au/ZrO_2 sample, formation of carbonate-like species took place only at the gold–support interface; these species supposedly migrated over the whole catalyst surface (but there was no evidence to support either inference). The IR band detected at 1230 cm^{-1} by Daté et al. [13] in the spectrum of Au/Al_2O_3 during CO oxidation catalysis was also observed when Al_2O_3 alone was exposed to CO_2. These authors correlated the intensity of this band inversely with the intensity of the gas-phase CO_2 band (at 2360 cm^{-1}) and concluded that the carbonate-like species were located at the Au–support interface and caused deactivation. However, we emphasize that accumulation of any kind of carbonate-like species takes substantial time to reach a maximum (for example, Smart et al. [35] detected increasing intensities of IR bands characterizing carbonate-like species on MgO for more than 6 h after introduction of CO into a batch IR cell), and Daté's experiment was carried out for less than an hour.

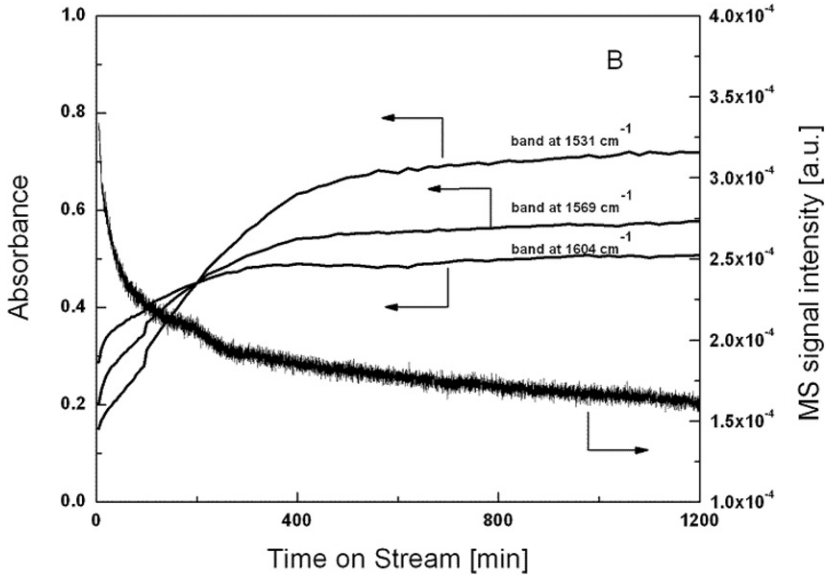

Fig. 10. Changes in intensity of mass spectral signal of CO_2 produced in CO oxidation catalysis correlated with changes in intensities of IR bands at 1604, 1569, and 1531 cm^{-1} observed during CO oxidation catalyzed by Au/MgO in a flow reactor. The catalyst was made by bringing $Au(CH_3)_2(acac)$ in contact with partially dehydroxylated MgO followed by treatment in flowing helium as the sample was heated to 473 K.

Thus, we regard the suggestions about catalyst deactivation associated with carbonate-like species as preliminary and do not rule out the possibility that the carbonate-like species observed by Daté corresponding to the 1230-cm^{-1} band was only a spectator.

In our work, we observed evidence of changes in the surface carbonate species during both catalyst activation and deactivation over longer periods. Although both CO and CO_2 adsorb on MgO alone to form various carbonate-like species, some new such species were identified by IR spectroscopy when gold was present on the MgO during exposure to CO and to CO_2 and during CO oxidation catalysis, as shown by the bands at 1606, 1566, 1534, 1343, 1315, and 1277 cm^{-1} (Fig. 6). Similar bands (at 1609, 1558, and 1526 cm^{-1}) were also detected by Manzoli et al. [50] on Au/ZnO during CO oxidation catalysis. The authors pointed out that they could be assigned either to a bidentate carbonate species bonded to metallic gold or to a carbonyl species σ-bonded to gold atoms and simultaneously π-bonded to support cations. They assigned the 1609-cm^{-1} band to the latter and did not provide a clear statement about the assignment of the 1558- and 1526-cm^{-1} bands, as the species represented by these bands were stable only in a narrow temperature range (90–170 K).

In contrast, in our case, the bands at 1604, 1569, 1531, 1338, 1315 and 1277 cm^{-1} were stable at 303 K and increased in intensity with time on stream during CO oxidation catalysis (as discussed below). Therefore, we assign them to carbonate-like species formed on gold, with the participation of $Au^{\delta+}$ sites providing the counter ions.

With increasing time on stream during CO oxidation catalysis, all the bands in the 1800–1000-cm^{-1} region were characterized by intensity changes. We discuss first the bands that were also observed on MgO alone. The intensity of the 1217-cm^{-1} band increased at a high rate, reaching its maximum within 10 min and decreasing thereafter. Because of superposition, the behavior of the contaminant bands is not evident. However, decreases in the intensity of the higher-frequency component of the band at approximately 1670 cm^{-1} and of a component at approximately 1380 cm^{-1} are clearly evident. Therefore, we infer that the accumulation of the bicarbonate species does not provide an explanation for the continuous activity loss for more than 600 min on stream during catalysis in a flow reactor. However, we cannot exclude the possibility that bicarbonate species are precursors of species causing activity loss (*vide supra*).

Next we discuss the bands at 1604, 1569, and 1531 cm^{-1}, which were observed for Au/MgO but not for MgO alone (the lower-frequency components are not considered here because of the superimposition with other strong bands in the region). The bands at 1604, 1569, and 1531 cm^{-1} increased slowly and continuously during the catalytic reaction in the flow reactor. A plot of their intensities versus time on stream shows that their increasing intensities track the decrease in intensity of the mass spectrometer signal for product CO_2 (Fig. 10), consistent with the inference that carbonate-like species formed on gold clusters block the active sites and are responsible for catalyst deactivation.

When the used catalyst was treated in helium at 473 K, the carbonate-like species were removed from the gold (as indicated by the IR spectra (Supplemental Information) and the mass spectrometric evidence of CO_2 formation (Fig. 2B)), and the catalyst regained activity. When it was then used again as a catalyst, it again lost activity, with the pattern (Fig. 2A) being similar to that of the first activation–deactivation cycle. The activity increased after each activation–deactivation cycle (Fig. 2A).

Thus, we infer that there is more to the story of catalyst deactivation than the influence of the carbonate-like species. The EXAFS data show that the average cluster size increased after three activation–deactivation cycles. Thus, we infer that aggregation of gold, which led to an increase in the average gold cluster diameter to a value of about 30 Å at the end of three activation–deactivation cycles (Table 1), led to an increase in the catalytic activity for CO oxidation. This result is consistent with the suggestion [57,58] that there is an optimum cluster diameter of about 25–30 Å) for CO oxidation catalysis. Gold clusters on MgO with an average diameter of about 30 Å were obtained previously through various treatments of the same as-prepared Au/MgO sample (mononuclear Au(III) species prepared by bringing $Au(CH_3)_2(acac)$ in contact with partially dehydroxylated MgO) [22,28], suggesting that they may be the stable gold species on MgO support.

The result that the deactivation caused by carbonate-like species is easily reversed, combined with the observation that the clusters formed after several reactivation steps are stable, indicates that the catalyst deactivation phenomena reported here should not be a major hindrance to applications of catalysts such as ours.

6. Conclusions

The Au/MgO catalyst made by bringing $Au(CH_3)_2(acac)$ in contact with partially dehydroxylated MgO was not active initially for CO oxidation at room temperature, but the sample was activated by treatment in flowing helium at 473 K, during which the original mononuclear Au(III) species decomposed as methyl ligands were lost and the gold was reduced and aggregated. XANES and EXAFS characterizations indicate that the treated sample contained clusters of gold that was essentially zerovalent.

The treated Au/MgO sample was active for CO oxidation catalysis at 303 K. However, it underwent rapid deactivation during the first hour of operation in a flow reactor, followed by slower deactivation for more than 10 h. IR spectra of the catalyst recorded under working conditions include several bands in the 1800–1000 cm^{-1} region, which arose from various carbonate-like species formed on the support and on gold. Intensities of the bands indicating carbonate-like species on MgO increased rapidly and reached maxima within 200 min on stream. In contrast, the intensities of the bands characterizing the carbonate-like species on gold continued to increase throughout the operation in the flow reactor, for 20 h. The intensities of these bands are correlated inversely with the conversion of CO to CO_2, consistent with the inference that they caused the catalyst deactivation.

The deactivated catalyst was reactivated by treatment in flowing helium, which led to removal of the carbonate-like species. The average gold cluster diameter increased after each deactivation-reactivation cycle, and the catalytic activity increased from one cycle to the next. The data indicate that the average gold cluster diameter in the catalyst after these cycles was about 30 Å.

Thus, the data presented here are the first to resolve the separate effects of carbonate-like species on the support, such species on the gold, and the average gold cluster size.

Although the XANES and EXAFS data suggest that the treated Au/MgO sample contained only zerovalent gold before and after the catalytic reaction, we cannot exclude the participation of cationic gold in the catalysis, as cationic gold species were indicated by IR spectra of the working catalyst. As in a previous investigation of an Au/La_2O_3 catalyst [48], the oxidizing agent for gold was found to be CO_2.

Acknowledgments

This work was supported by U.S. Department of Energy (Grant FG02-04ER15513), the Alexander von Humboldt Foundation (AvH fellowship to M.M.), and a NATO Collaborative Linkage Grant (PST.CLG 980289). K.H., E.I., and M.M. also acknowledge support from the Bulgarian Scientific Foundation (project VUX-303). We acknowledge the National Synchrotron Light Source (NSLS) and the Stanford Synchrotron Radiation Laboratory (SSRL) for access to beam time. We thank the staffs of NSLS and SSRL for assistance.

Supplemental Information

The online version of this article contains additional supplemental information.

Please visit DOI: 10.1016/j.jcat.2008.11.005.

References

[1] M. Haruta, S. Tsubota, T. Kobayashi, H. Kageyama, M.J. Genet, B. Delmon, J. Catal. 144 (1993) 175.
[2] M.M. Schubert, S. Hackenberg, A.C. van Veen, M. Muhler, V. Plzak, R.J. Behm, J. Catal. 197 (2001) 113.
[3] F. Boccuzzi, A. Chiorino, M. Manzoli, P. Lu, T. Akita, S. Ichikawa, M. Haruta, J. Catal. 202 (2001) 256.
[4] M. Daté, M. Okumura, S. Tsubota, M. Haruta, Angew. Chem. Int. Ed. 43 (2004) 2129.
[5] H.-S. Oh, J.H. Yang, C.K. Costello, Y.M. Wang, S.R. Bare, H.H. Kung, M.C. Kung, J. Catal. 210 (2002) 375.
[6] J.C. Fierro-Gonzalez, B.C. Gates, J. Phys. Chem. B 108 (2004) 16999.
[7] J. Steyn, G. Pattrick, M.S. Scurrell, D. Hildebrandt, M. Raphulu, E. van der Lingen, Catal. Today 122 (2007) 254.
[8] F. Moreau, G.C. Bond, Top. Catal. 44 (2007) 95.
[9] F. Moreau, G.C. Bond, Catal. Today 114 (2006) 362.
[10] K.Y. Ho, K.L. Yeung, Gold Bull. 40 (2007) 15.
[11] M. Azar, V. Caps, F. Morfin, J.-L. Rousset, A. Piednoir, J.-C. Bertolini, L. Piccolo, J. Catal. 239 (2006) 307.
[12] M.M. Shubert, A. Venugopal, M.J. Kahlich, V. Plzak, R.J. Behm, J. Catal. 222 (2004) 32.
[13] M. Daté, H. Imai, S. Tsubota, M. Haruta, Catal. Today 122 (2007) 222.
[14] F. Boccuzzi, G. Ghiotti, A. Chiorino, Surf. Sci. 162 (1985) 361.
[15] P. Konova, A. Naydenov, T. Tabakova, D. Mehandjiev, Catal. Commun. 5 (2004) 537.
[16] P. Konova, A. Naydenov, Cv. Venkov, D. Mehandjiev, D. Andreeva, T. Tabakova, J. Mol. Catal. A 213 (2004) 235.
[17] C.K. Costello, M.C. Kung, H.-S. Oh, Y. Wang, H.H. Kung, Appl. Catal. A 232 (2002) 159.
[18] C.K. Costello, J.H. Yang, H.Y. Law, Y. Wang, J.-N. Lin, L.D. Marks, M.C. Kung, H.H. Kung, Appl. Catal. A 243 (2003) 15.
[19] M.M. Shubert, V. Pizak, J. Garche, R.J. Behm, Catal. Lett. 76 (2001) 143.
[20] M. Moreau, G.C. Bond, B. van der Linden, B.A.A. Silberova, M. Makkee, Appl. Catal. A 347 (2008) 208.
[21] L.H. Little, Infrared Spectra of Adsorbed Species, Academic Press, London, 1966, p. 74.
[22] J. Guzman, B.C. Gates, Angew. Chem. Int. Ed. 42 (2003) 690.
[23] G. Kunzmann, Doctoral thesis, University of Munich, 1987.
[24] M. Vaarkamp, J.C. Linders, D.C. Koningsberger, Physica B 209 (1995) 159.
[25] E.A. Stern, Phys. Rev. B 48 (1993) 9825.
[26] A.L. Ankudinov, J.J. Rehr, Phys. Rev. B 56 (1997) R1712.
[27] D.C. Koningsberger, B.L. Mojet, G.E. van Dorssen, D.E. Ramaker, Top. Catal. 10 (2000) 143.
[28] J. Guzman, B.G. Anderson, C.P. Vinod, K. Ramesh, J.W. Niemantsverdriet, B.C. Gates, Langmuir 21 (2005) 3675.
[29] J.C. Fierro-Gonzalez, B.C. Gates, J. Phys. Chem. B 109 (2005) 7275.
[30] S. Galvano, G. Parravano, J. Catal. 55 (1978) 178.
[31] A. Zwijnenburg, A. Goossens, W.G. Sloof, M.W.J. Crajé, A.M. van der Kraan, L.J. de Jongh, M. Makkee, J.A. Moulijin, J. Phys. Chem. B 106 (2002) 9853.
[32] J. Guzman, B.C. Gates, J. Phys. Chem. B 106 (2002) 7659.
[33] J.T. Calla, R.J. Davis, J. Phys. Chem. B 109 (2005) 2307.
[34] A. Jentys, Phys. Chem. Chem. Phys. 1 (1999) 4059.
[35] R.S.C. Smart, T.L. Slager, L.H. Little, R.G. Greenler, J. Phys. Chem. 77 (1973) 1019.
[36] G. Spoto, E.N. Gribov, G. Ricchiardi, A. Damin, D. Scarano, S. Bordiga, C. Lamberti, A. Zecchina, Prog. Surf. Sci. 76 (2004) 71.
[37] A. Zecchina, S. Coluccia, G. Spoto, D. Scarano, L. Marchese, J. Chem. Soc. Faraday Trans. 86 (1990) 703.
[38] T. Tashiro, J. Ito, R.-B. Sim, K. Miyazawa, E. Hamada, K. Toi, J. Phys. Chem. 99 (1995) 6115.
[39] D.G. Rethwisch, J.A. Dumesic, Langmuir 2 (1986) 73.
[40] J.I. Di Cosimo, V.K. Diez, M. Xu, E. Iglesia, C.R. Apesteguia, J. Catal. 178 (1998) 499.
[41] G.A.H. Mekhemer, S.A. Halawy, M.A. Mohamed, M.I. Zaki, J. Phys. Chem. B 108 (2004) 13379.
[42] C. Li, G. Li, Q. Xin, J. Phys. Chem. 98 (1994) 1933.
[43] G. Busca, V. Lorenzelli, Mater. Chem. 7 (1982) 89.
[44] K. Hadjiivanov, G. Busca, Langmuir 10 (1994) 4534.
[45] M. Mihaylov, H. Knözinger, K. Hadjiivanov, B.C. Gates, Chem. Ing. Tech. 79 (2007) 795.
[46] F. Boccuzzi, A. Chiorino, M. Manzoli, Surf. Sci. 454–456 (2000) 942.
[47] A.S. Wörz, U. Heiz, F. Cinquini, G. Pacchioni, J. Phys. Chem. B 109 (2005) 18418.
[48] M. Mihaylov, E. Ivanova, Y. Hao, K. Hadjiivanov, B.C. Gates, H. Knözinger, Chem. Commun. (2008) 175.
[49] M. Mihaylov, B.C. Gates, J.C. Fierro-Gonzalez, K. Hadjiivanov, H. Knözinger, J. Phys. Chem. C 111 (2007) 2548.
[50] M. Manzoli, A. Chiorino, F. Boccuzzi, Appl. Catal. B 52 (2004) 259.
[51] J.D. Henao, T. Caputo, J.H. Yang, M.C. Kung, H.H. Kung, J. Phys. Chem. B 110 (2006) 8689.
[52] M. Mihaylov, J.C. Fierro-Gonzalez, H. Knözinger, B.C. Gates, K. Hadjiivanov, J. Phys. Chem. B 110 (2006) 7695.
[53] M. Okumura, S. Nakamura, S. Tsubota, T. Nakumura, M. Azuma, M. Haruta, Catal. Lett. 51 (1998) 53.
[54] N. Weiher, E. Bus, L. Delannoy, C. Louis, D.E. Ramarker, J.T. Miller, J.A. van Bokhoven, J. Catal. 240 (2006) 100.
[55] D. Tibiletti, A. Amieiro-Fonseca, R. Burch, Y. Chen, J.M. Fisher, A. Goguet, C. Hardacre, P. Hu, D. Thompsett, J. Phys. Chem. B 109 (2005) 22553.
[56] G.N. Vayssilov, B.C. Gates, N. Rösch, Angew. Chem. Int. Ed. 42 (2003) 1391.
[57] R. Grisel, K.-J. Weststrate, A. Gluhoi, E. Nieuwenhuys, Gold Bull. 35 (2002) 39.
[58] G.R. Bamwenda, S. Tsubota, T. Nakamura, M. Haruta, Catal. Lett. 44 (1997) 83.